Ecological resource competition as a driver of metallome evolution

Authors:
Morgan S. Sobol[1], Holly R. Rucker[1], Eric Libby[2], Betül Kaçar[1*] and Ariel D. Anbar[3*]

[1]Department of Bacteriology, University of Wisconsin-Madison, Madison, WI, USA

[2]Department of Mathematics and Mathematical Statistics, Umeå University, Umeå, Sweden

[3]School of Earth and Space Exploration and School of Molecular Sciences, Arizona State University, AZ, Tempe, USA

*Correspondence should be addressed to Betül Kaçar (bkacar@wisc.edu) or Ariel Anbar (anbar@asu.edu).

Keywords:
nitrogenase, molecular paleobiology, GOE, Proterozoic, molybdenum, metallome, resource competition

Classification: Biological Sciences - Evolution, Earth Sciences: Geochemistry, Paleobiology

Significance statement

The selection of metals in biochemical evolution is widely attributed to either the relative environmental availability of specific metals or their functional benefits in biological systems. We propose a third pressure, ecological resource competition, which is typically overlooked as a driver of molecular novelty in deep time. Specifically, we hypothesize that competition between Mo-dependent nitrogen-fixing prokaryotes and Mo-dependent nitrate reducers led to the emergence of Mo-free “alternative” nitrogenase enzymes during the early Proterozoic. This novel hypothesis explains the paradoxical emergence of alternative nitrogenases after the Great Oxidation Event despite increasing ocean Mo abundances at that time. Competition among microbial species for the same metals likely drove molecular innovations, especially in response to dynamically changing geochemical landscapes.

Abstract

Undoubtedly, Earth's first redox revolution, which culminated ~2.4 billion years ago in the Great Oxidation Event (GOE), fundamentally altered the resources available to microbial communities, leading to novel ecological competitions and evolutionary innovations. These eco-evolutionary dynamics are largely unexplored, particularly at the molecular level. Here, we hypothesize that such dynamics in the wake of the GOE explain the otherwise paradoxical evolutionary history of metal use in nitrogen fixation by nitrogenase. This ancient metalloenzyme exists in three isozymes, with distinct metal cofactors. Recent research demonstrates that the most ancient isozyme, emerging a billion years or more before the GOE, required a molybdenum (Mo)-based cofactor. "Alternative" nitrogenases using iron (Fe) or vanadium (V) cofactors evolved after the GOE. This history is puzzling because Mo availability in the environment *increased* after the GOE, while Fe availability *decreased*, due to the contrasting environmental redox behaviors of these elements. Why, then, did the alternatives emerge only after the GOE? Using a simple model constrained by known microbial Mo quotas, we demonstrate that a strong selection pressure for use of metals in nitrogenase other than Mo is a likely consequence of competition between nitrogen-fixing prokaryotes and nitrate-reducing microbes, which require Mo for nitrate reduction and assimilation. This competition would have intensified after the GOE due to increasing environmental availability of nitrate, explaining the evolutionary timing of the nitrogenase isozymes. Ecological resource competition therefore emerges as a third driver of metallome evolution in deep-time, alongside the relative environmental availabilities and adaptive advantages of particular metals.

Introduction

Element use in biology is intricately linked to element availability in the surrounding environment. Consequently, metalloenzyme evolution and biological stoichiometry are broadly thought to have been shaped by changes in environmental availabilities throughout Earth's history (1–4). However, the chemical characteristics of an element that make it biochemically useful also affect element selection, leading to selection pressures

that can be in tension with availability (5). A third possible driver in the evolution of metal-containing biomolecules within a biological system (i.e., the metallome) is largely unexplored: resource competition, and its impact on organismal interaction and community composition (5).

The importance of resource competition may be seen in the evolution of biological nitrogen fixation and the enzyme “nitrogenase”, which arose by the mid-Archean (6–9). All life depends on this biological process and thus on nitrogenase, through which nitrogen enters the biosphere by being “fixed” from N_2 into a chemically reduced form that can be used to build new nucleic acids, proteins, and other biomolecules (10). Nitrogenase is a metalloenzyme existing in three distinct isoforms, containing either molybdenum and iron (“Mo-nitrogenase"), vanadium and iron (“V-nitrogenase”), or only iron (“Fe-nitrogenase") (**Figure 1A** and **B**). Today, Mo-nitrogenase is the most abundant form; the Mo-independent nitrogenases are collectively termed "alternative" nitrogenases (11–13). Parsimony may suggest that the metal preferences of nitrogenases were shaped primarily by changes in environmental availability, whereby the biosphere optimized around the most abundant metal at its disposal at a given time on an evolving planet. If so, Fe-nitrogenase would be ancestral because Earth’s oceans at the time of nitrogenase’s emergence were O_2-free and hence replete with Fe (14–16), while Mo was likely scarce (17). However, geochemical and evolutionary studies independently indicate that ancestral nitrogenases favored Mo (7, 18, 19) (**Figure 1C**). Phylogenetic reconstructions further suggest that alternative nitrogenases emerged through an ancient subfunctionalization of a Mo-nitrogenase at least 1 billion years later (8, 20) (**Figure 1A** and **1C**), and through the acquisition of characteristic sequence novelties (i.e., the G subunit) (21) whose birth coincides with the approximate timing of the Great Oxidation Event (GOE) (9, 20–23).

The early emergence of Mo-nitrogenase despite Mo scarcity in Archean oceans can be understood in terms of the particular chemical characteristics that make Mo-nitrogenase the most efficient of the nitrogenase isozymes (12, 24, 25). However, the emergence of the Mo-free alternatives after the GOE remains paradoxical: Why would the less efficient Mo-free alternative nitrogenases evolve during a time when Mo availability *increased*, and

Fe availability *decreased*? What evolutionary pressures drove the diversification and selection for alternative nitrogenase metal cofactors at that time?

We propose that the complex evolutionary history of the nitrogenases is best explained by ecological resource competition. Although our current understanding of resource competition offers valuable insights into modern microbial ecology (26, 27), its role is often overlooked in studies of early microbial life.

Our hypothesis builds on observations suggesting that nitrate (NO_3^-) concentrations in surface oceans increased after the GOE, alongside Mo (28–31). The increased availability of NO_3^- and Mo together favored the ecological radiation of NO_3^--reducing microbes, including both prokaryotes and eukaryotes, which use another Mo-dependent enzyme: NO_3^--reductase (32). Genes utilized in NO_3^- reduction are inferred to have arisen around the time of the GOE (2.8-2.3 Ga) (9) (**Figure 1C**). We propose that the competition for Mo between diazotrophs and these NO_3^--reducers—which emerged between 2.8 – 1.0 Ga (9, 33–39)—generated a selection pressure that drove the evolution, and subsequent diversification of Mo-independent alternative nitrogenases.

To evaluate this hypothesis quantitatively, we consider an ecological model that describes the competition dynamics between diazotrophs and a NO_3^--reducing eukaryote that assimilates NO_3^-.

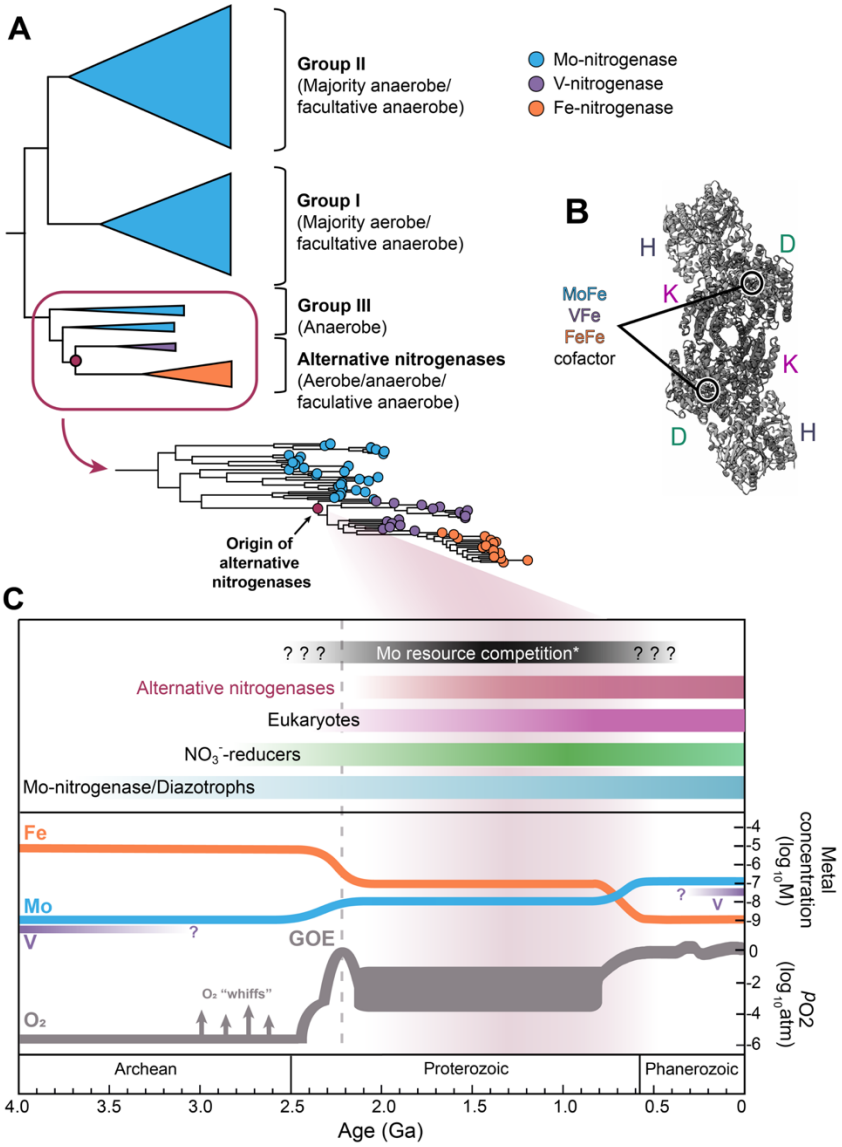

Figure 1. Key evolutionary events surrounding the evolution of alternative nitrogenases. **A)** Evolutionary history of nitrogenase based on maximum-likelihood phylogenetic construction of nitrogenase structural genes HDK (8) with aerobic, anaerobic, and facultative clades highlighted. Node distances are not to scale. **B)** Structure of the *Azotobacter vinelandii* Mo-nitrogenase complex (HDK) (40) and the three metal cofactors that different nitrogenase isozymes variably incorporate (Mo, V, and Fe) (41–43). **C)** Estimated age of alternative nitrogenases coincides with the Great Oxidation Event (GOE), and consequent changes in Mo, V, and Fe availabilities. The era of hypothesized competition for Mo between diazotrophs and ancestral NO_3^--reducers (black bar) presumably began prior to the GOE, when evidence of ocean oxygenation appears (44), and persisted until pervasive environmental oxygenation led to a sharp rise of Mo ocean availability in the Neoproterozoic (45). Atmospheric O_2 partial pressure estimates through time are from (46). Ocean metal abundances for Mo and Fe are from (47). Vanadium availability is estimated from (48, 49). Nitrogenase age estimates are based on geological nitrogen isotope signatures (7), evolutionary rate analysis (20), and molecular clock analysis (9, 22). Time-range for NO_3^--reducers is based on molecular clock analysis (9) and geological nitrogen isotope signatures (7, 50). The time-range for eukaryotes is based on molecular clock analyses and fossil evidence (34, 35, 37, 38).

Results and Discussion

To perform a first-order quantitative test of our hypothesis, we adapt the Monod model, originally created by Jacques Monod in the 1940s to model microbial growth under a limiting resource (51). This framework is used widely in ecological modeling (52). Specifically, we consider a simple system in which populations of diazotrophs (*D*) and NO_3^--assimilators (*A*) cohabitate and compete for Mo (**Figure 2A, Supplemental Table 1**).

Here, we focus on algae as the selected representative of NO_3^--assimilators because extensive data is available on their Mo requirements (53), and because the emergence of eukaryotes as NO_3^--assimilators would have significantly impacted diazotrophs by increasing the competition for Mo.

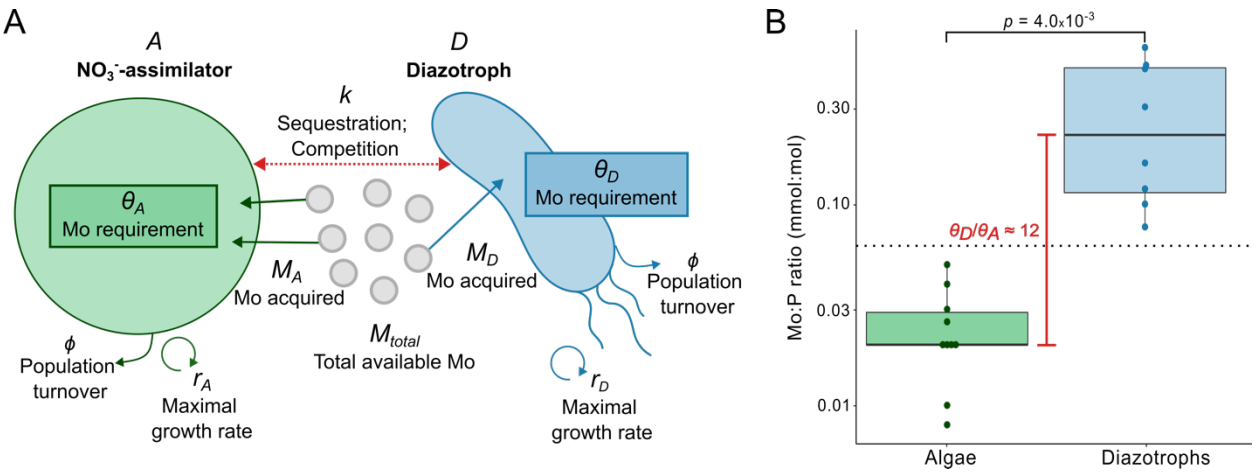

Figure 2. Overall components of the proposed competition model.
A) Mo is required by both NO_3^--assimilators and N_2-fixing prokaryotes (diazotrophs), thus in our model Mo (*M*) is the limiting factor for growth of the populations of both NO_3^--assimilators (*A*) and diazotrophs (*D*). Both species have their respective requirements for Mo ($\theta_A$or θ_D) and a maximal potential growth rate (r_A or r_D). To determine the amount of Mo acquired by each species (M_A or M_D), total available Mo (M_{total}) is partitioned across the populations based on each organism's relative abundance and relative ability to sequester Mo (parameter *k*). Phi (ϕ) is the loss rate parameter to account for population turnover. Competition dynamics between NO_3^--assimilators and diazotrophs can therefore be analyzed in terms of differences in their Mo dependency, maximal growth rates, and their ability to sequester Mo. **B)** Empirical estimates of Mo requirements from extant diazotrophs (blue) and algae (green), our model NO_3^--assimilators, were compared. Diazotrophs require significantly more Mo than NO_3^--assimilators on average. We estimated the median Mo requirement ratio between diazotrophs and NO_3^--assimilators to be $(\theta_D/\theta_A) \approx 12$ (red solid line). The black dotted line represents the midpoint between diazotrophs' lowest Mo:P (mmol:mol) and NO_3^--assimilator's highest. The y-axis is presented on a $\log_{10}$ scale to better visualize differences across orders of magnitude. Data can be found in Supplemental Table 2.

The modeled system (**Figure 2A**) considers that the total Mo pool (M_{total}) from which both diazotrophs and NO_3^--assimilators draw is fixed at some constant amount. We assume that diazotrophs and NO_3^--assimilators each have their own Mo requirements for growth (θ_D and θ_A, respectively). Maximal growth rates (r_D or r_A) represent the theoretical highest growth rate that either species can achieve under ideal conditions. They serve as a benchmark, reflecting the potential for growth if Mo requirements (θ_D and θ_A) are fully met. Population turnover (ϕ), or a population's removal from the environment, is assumed to be the same for both species, following traditional simplified resource-competition models (54–57). The allocation of Mo between the two species is therefore represented as a competition whereby the total Mo pool is shared between the two species based on their population sizes and relative competitive ability (k) to sequester Mo, i.e. their effectiveness in capturing Mo for their private use. Thus, as the populations of NO_3^--assimilators and diazotrophs change over time, the fraction of Mo used by each species (M_D or M_A) also changes, altering their realized growth rates and subsequent survival. We use the form of a Monod equation $\frac{r_{cell}}{M_{cell}+\theta}$ (51) to describe the realized growth rates of diazotroph and NO_3^--assimilator populations as a function of the supply of Mo per cell ($M_{cell,D}$ and $M_{cell,A}$).

To determine M_D or M_A, we partition M_{total} across the two species' populations depending on their relative abundances and the competition parameter k, which represents how much more Mo diazotrophs can sequester relative to algae. Thus, the total amount of Mo used by diazotrophs (M_D) and NO_3^--assimilators (M_A) can be described as:

$$M_D = M_{total}\left(\frac{k\,D}{k\,D+A}\right) \quad [1]$$

$$M_A = M_{total}\left(\frac{A}{k\,D+A}\right) \quad [2]$$

When $k = 1$, both species are equally matched in their ability to sequester Mo and so the total amount of Mo is distributed based on the fraction of each species in the population. Alternatively, when $k > 1$, diazotrophs can sequester more of the Mo supply. The inverse is true when $k < 1$. The amount of Mo per cell (M_{cell}) is then the amount sequestered by diazotrophs (M_D) or algae (M_A) divided by the total population of each species (D or A),

such that $M_{cell,D}$ = M_D/D and $M_{cell,A}$ = M_A/A. Based on these considerations, we describe the population dynamics of *D* and *A* over time using a system of differential equations:

$$\frac{dD}{dt} = r_D \frac{M_{cell,D}}{M_{cell,D} + \theta_D} D - \phi D \quad [3]$$

$$\frac{dA}{dt} = r_A \frac{M_{cell,A}}{M_{cell,A} + \theta_A} A - \phi A \quad [4]$$

Within this system, the absence of one species allows the other species to grow to its carrying capacity, described by $\frac{(r_D-\phi)M_{total}}{\phi\theta_D}$ for *D* or $\frac{(r_A-\phi)M_{total}}{\phi\theta_A}$ for *A*. The carrying capacity for each species is determined when their growth is at equilibrium ($\frac{dD}{dt}$ = 0 for *D* and $\frac{dA}{dt}$ = 0 for *A*). When both species are present, competition for Mo results in one species driving the other to extinction, except for a very specific combination of parameters whereby the two species are equally competitive:

$$k = \left(\frac{\theta_D}{\theta_A}\right)\frac{(r_A - \phi)}{(r_D - \phi)} \quad [5]$$

If $k > \left(\frac{\theta_D}{\theta_A}\right)\frac{(r_A - \phi)}{(r_D - \phi)}$, diazotrophs drive NO_3^--assimilators to extinction, whereas if $k < \left(\frac{\theta_D}{\theta_A}\right)\frac{(r_A - \phi)}{(r_D - \phi)}$, diazotrophs go extinct. The outcome of the competition therefore depends on three parameters: 1) the ratio of dependencies on Mo ($\frac{\theta_D}{\theta_A}$); 2) the ratio of maximal growth rates $\frac{(r_A - \phi)}{(r_D - \phi)}$; and 3) *k*.

To determine the ratio of Mo requirements (θ_D/θ_A), we refer to prior studies that reported measured cellular Mo concentrations in diazotrophs (53, 58–60) and in algal NO_3^--assimilators (53) grown with approximately the same Mo concentration (~100 nM) (**Figure 2B; Supplemental Table 2**). For more straightforward comparisons, the Tuit *et al.* (2004) data (58) was normalized to average cellular phosphorus (P) concentrations (**Supplemental Table 3**) based on Redfield stoichiometry (61). Normalized cellular Mo concentrations (reported as mmol Mo : mol P) are 0.077 - 0.6 for diazotrophs, whereas for algae they range from 0.008 - 0.05. Thus, the average Mo:P in diazotroph cells is

approximately an order of magnitude higher than in algae (one-tail *p*-value=4.0 x 10^{-3}; **Supplemental Table 4**).

In general, cellular concentrations of Mo in diazotrophs agree with estimates of nitrogenase Mo requirements in whole cells (58, 60). Although analogous estimates for NO_3^--reducers are not available, the empirical differences in Mo requirements between diazotrophs and algae can likely be attributed to differences in the catalytic reaction rates of their respective molybdoenzymes (62, 63). The data in **Figure 2B** are therefore consistent with previous estimates that diazotrophs require 125 times more Mo per cell than NO_3^--assimilators to achieve the same specific rate of N assimilation (mol N assimilated per mol Mo s^{-1}) (62, 63). *Azotobacter vinelandii* and *Trichodesmium erythraeum* are exceptions, in that they are diazotrophs that are known to sequester Mo in excess of their N_2-fixation needs by up to 10x and 5x, respectively (58, 60). However, even after accounting for this additional Mo storage, their cellular Mo concentrations remain higher than those of most NO_3^--assimilators (**Supplemental Table 2**). The higher Mo requirements of diazotrophs underscores their metabolic constraints when they seek to operate nitrogenase at its full catalytic capacity to meet N_2-fixation demands.

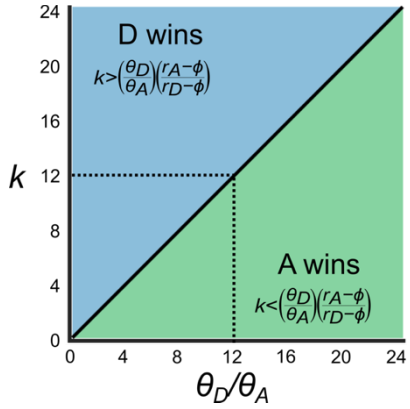

Figure 3. Mo competition model outcome. Competition dynamics based on differences in Mo requirements (θ_D/θ_A) and amount of Mo sequestered (*k*) between NO_3^--assimilators (*A*) and diazotrophs (*D*). The estimated ratio of specific Mo requirements of diazotrophs relative to algae (θ_D/θ_A) is ~ 12 (black dotted lines), as suggested by the empirical data assembled here. When the growth rates for NO_3^--assimilators and diazotrophs are the same, the ratio of θ_D/θ_A to *k* can be described as a proportional relationship that determines who wins the competition. In other words, when θ_D/θ_A is equal to 12, then diazotrophs need to sequester at least 12x more Mo than NO_3^--assimilators in order to survive. As the relative Mo requirement decreases (moving left on the x-axis), the "win condition" for diazotrophs can be achieved with smaller values of *k*, reducing the need for highly efficient Mo sequestration. As long as diazotrophs do not have a net maximal growth rate that is 12x greater than NO_3^--assimilators, the same logic applies. The evolution of alternative nitrogenases is therefore a probable strategy to cope with competition for Mo.

Using our estimate for Mo requirements from **Figure 2B** (θ_D/θ_A ~ 12) we focus the outcome of the competition on the relative sequestration of Mo that would be required for diazotrophs to survive when the net maximal growth rate is the same for both species ($\frac{(r_A - \phi)}{(r_D - \phi)} = 1$) (**Figure 3**).

When maximal growth rates are equal, the competition outcome is directly determined by the Mo requirements. In this scenario, diazotrophs would need to sequester at least 12 times more Mo than NO_3^--assimilators in order to survive. The dependence of diazotrophs on efficient sequestration (*k*) can be alleviated if they are able to reduce their high Mo requirement (i.e. moving left along the x-axis in **Figure 3**). This logic applies under different growth rate scenarios, unless the net maximal growth rate of the diazotroph is 12x greater than that of the NO_3^--assimilator. It is not likely that diazotrophs would achieve such high rates when the two species cohabitate as previous models and experimental work suggest that diazotroph growth rates are lower than or comparable to those of non-diazotrophic phytoplankton (55, 56, 64–66). Thus, the central message is reinforced: diazotrophs face severe competitive pressure due to their high Mo demands, regardless of growth rate differences. This relationship constitutes a selection pressure favoring the evolution of Mo-free, alternative nitrogenases.

Our ability to extend this model to all NO_3^- reducers is limited by the paucity of comparable Mo data for both dissimilatory and assimilatory NO_3^- reducers. The Mo requirements for different NO_3^- reductases are suggested to be influenced by variations in enzyme structure and active site configuration (67). However, the extent to which these properties impact overall cellular Mo requirements is poorly understood. Investigating whether the Mo requirements of NO_3^- assimilators can be broadly extrapolated to NO_3^- reducers should be a focus for future research.

Our findings mathematically illustrate a key prediction of resource-ratio theory (54, 68): That species with lower resource requirements have a competitive advantage in resource-limited environments. This competition dynamic becomes especially relevant when considering the evolutionary pressures faced by diazotrophs in ancient Mo-limiting environments. As NO_3^- availability in the oceans increased during the Proterozoic, fueling

266 the emergence and ecological advancement of Mo-using NO_3^--reducers, competition for
267 Mo likely intensified, disadvantaging diazotrophs that depended solely on Mo-nitrogenase
268 and hence favoring the evolution of alternative nitrogenases. This ancient resource
269 competition left a lasting imprint at the molecular level, where alternative nitrogenases
270 and Mo-sequestration strategies persist today (69–75). Most likely, alternative
271 nitrogenases continue to provide a competitive advantage in these settings, functioning
272 as "backup" enzymes in Mo-limited environments.

273 This study focuses on the consequences of ecological resource competition for the
274 evolutionary origins of nitrogenase isozymes. Nitrogenase evolution is unique only in that
275 we now have considerable knowledge about the timing of the evolution of metal usage in
276 this enzyme family, alongside approximate contemporaneous changes in global ecology
277 and the environmental availability of Mo. It is likely, however, that resource dynamics,
278 including ecological resource competition as highlighted here, also played a significant
279 role in shaping the evolution of other metalloenzymes, as resource competition is a
280 fundamental driver of microbial interactions and evolution (27). Much remains to be
281 uncovered about the integrated molecular, ecological, and geochemical histories of the
282 metallome (5). Addressing this knowledge gap will be essential to advance our
283 understanding of the co-evolution of Earth and life.

284

285 **Methods**

286 We obtained normalized cellular Mo:P data from the literature of cultures grown with
287 approximately 100 nM of Mo for comparison (**Supplemental Table 2**). P is often
288 measured simultaneously with metals (76), and so measured P data were used in these
289 cases. When only C-normalized Mo quotas were provided, P-normalized quotas were
290 calculated (**Supplemental Table 3**) using the Redfield ratio ($C_{106}N_{16}P$) (61). Statistical
291 differences between diazotroph and algae Mo requirements were determined using the
292 two-sample *t*-test assuming unequal variances with an alpha value of 0.05
293 (**Supplemental Table 4**).

294
295

Acknowledgments

This work was supported by the NASA Interdisciplinary Consortium for Astrobiology Research: Metal Utilization and Selection Across Eons, MUSE [80NSSC17K0296] with additional support from the NASA Exobiology Program [NNH23ZDA001N] and the USDA-NIFA Hatch Grant. M.S. is supported by the NASA Postdoctoral Program, administered by Oak Ridge Associated Universities under contract with NASA. We thank Yang Kuang for extensive conversations during the development of an earlier version of this manuscript. We also thank Evrim Fer, Kaustubh Amritkar, as well as the members of the MUSE ICAR team for their valuable feedback.

References

1. A. L. Zerkle, Biogeochemical signatures through time as inferred from whole microbial genomes. *Am. J. Sci.* **305**, 467–502 (2005).

2. C. L. Dupont, A. Butcher, R. E. Valas, P. E. Bourne, G. Caetano-Anollés, History of biological metal utilization inferred through phylogenomic analysis of protein structures. *Proc. Natl. Acad. Sci. U. S. A.* **107**, 10567–10572 (2010).

3. E. K. Moore, B. I. Jelen, D. Giovannelli, H. Raanan, P. G. Falkowski, Metal availability and the expanding network of microbial metabolisms in the Archaean eon. *Nat. Geosci.* **10**, 629–636 (2017).

4. H. Eom, W. J. Song, Emergence of metal selectivity and promiscuity in metalloenzymes. *J. Biol. Inorg. Chem.* **24**, 517–531 (2019).

5. K. I. Rico, A. K. Garcia, M. A. Saito, B. Kaçar, A. D. Anbar, “Mysteries of metallome evolution: Integrating insights from the Earth and life sciences” in *Treatise on Geochemistry*, A. Anbar, D. Weis, Eds. (Elsevier, 2025), pp. 337–364.

6. R. Navarro-González, C. P. McKay, D. N. Mvondo, A possible nitrogen crisis for Archaean life due to reduced nitrogen fixation by lightning. *Nature* **412**, 61–64 (2001).

7. E. E. Stüeken, R. Buick, B. M. Guy, M. C. Koehler, Isotopic evidence for biological nitrogen fixation by molybdenum-nitrogenase from 3.2 Gyr. *Nature* **520**, 666–669 (2015).

8. A. K. Garcia, H. McShea, B. Kolaczkowski, B. Kaçar, Reconstructing the evolutionary history of nitrogenases: Evidence for ancestral molybdenum-cofactor utilization. *Geobiology* **18**, 394–411 (2020).

9. C. Parsons, E. E. Stüeken, C. J. Rosen, K. Mateos, R. E. Anderson, Radiation of nitrogen-metabolizing enzymes across the tree of life tracks environmental transitions in Earth history. *Geobiology* **19**, 18–34 (2021).

10. H. R. Rucker, B. Kaçar, Enigmatic evolution of microbial nitrogen fixation: insights from Earth’s past. *Trends Microbiol.* **32**, 554–564 (2024).

11. P. E. Bishop, R. D. Joerger, Genetics and molecular biology of alternative nitrogen fixation systems. *Annu. Rev. Plant Physiol. Plant Mol. Biol.* **41**, 109–125 (1990).

12. R. R. Eady, Structureminus signFunction relationships of alternative nitrogenases. *Chem. Rev.* **96**, 3013–3030 (1996).

13. F. Mus, A. B. Alleman, N. Pence, L. C. Seefeldt, J. W. Peters, Exploring the alternatives of biological nitrogen fixation. *Metallomics* **10**, 523–538 (2018).

14. H. D. Holland, The oceans; A possible source of iron in iron-formations. *Econ. Geol.*

68, 1169–1172 (1973).

15. B. Kendall, A. D. Anbar, A. Kappler, K. O. Konhauser, “The Global Iron Cycle” in *Fundamentals of Geobiology*, (John Wiley & Sons, Ltd, 2012), pp. 65–92.

16. T. K. Lowenstein, B. Kendall, A. D. Anbar, “The geologic history of seawater” in *Treatise on Geochemistry*, H. D. Holland, K. K. Turekian, Eds. (Elsevier, 2014), pp. 569–622.

17. A. D. Anbar, A. H. Knoll, Proterozoic ocean chemistry and evolution: a bioinorganic bridge? *Science* **297**, 1137–1142 (2002).

18. X. Zhang, D. M. Sigman, F. M. M. Morel, A. M. L. Kraepiel, Nitrogen isotope fractionation by alternative nitrogenases and past ocean anoxia. *Proc. Natl. Acad. Sci. U. S. A.* **111**, 4782–4787 (2014).

19. A. K. Garcia, *et al.*, Nitrogenase resurrection and the evolution of a singular enzymatic mechanism. *Elife* **12** (2023).

20. E. S. Boyd, T. L. Hamilton, J. W. Peters, An alternative path for the evolution of biological nitrogen fixation. *Front. Microbiol.* **2**, 205 (2011).

21. B. Cuevas-Zuviría, *et al.*, Emergence of an orphan nitrogenase protein following atmospheric oxygenation. *Mol. Biol. Evol.* **41** (2024).

22. H.-W. Pi, Y.-R. Chiang, W.-H. Li, Mapping geological events and nitrogen fixation evolution onto the timetree of the evolution of nitrogen-fixation genes. *Mol. Biol. Evol.* **41** (2024).

23. B. Kaçar, Reconstructing early microbial life. *Annu. Rev. Microbiol.* **78**, 463–492 (2024).

24. J. A. Rees, *et al.*, Comparative electronic structures of nitrogenase FeMoco and FeVco. *Dalton Trans.* **46**, 2445–2455 (2017).

25. D. F. Harris, *et al.*, Mechanism of N2 reduction catalyzed by Fe-nitrogenase involves reductive elimination of H2. *Biochemistry* **57**, 701–710 (2018).

26. M. E. Hibbing, C. Fuqua, M. R. Parsek, S. B. Peterson, Bacterial competition: surviving and thriving in the microbial jungle. *Nat. Rev. Microbiol.* **8**, 15–25 (2010).

27. M. Ghoul, S. Mitri, The ecology and evolution of microbial competition. *Trends Microbiol.* **24**, 833–845 (2016).

28. E. E. Stüeken, M. A. Kipp, M. C. Koehler, R. Buick, The evolution of Earth’s biogeochemical nitrogen cycle. *Earth Sci. Rev.* **160**, 220–239 (2016).

29. A. L. Zerkle, *et al.*, Onset of the aerobic nitrogen cycle during the Great Oxidation Event. *Nature* **542**, 465–467 (2017).

30. M. A. Kipp, E. E. Stüeken, M. Yun, A. Bekker, R. Buick, Pervasive aerobic nitrogen cycling in the surface ocean across the Paleoproterozoic Era. *Earth Planet. Sci. Lett.* **500**, 117–126 (2018).

31. G. Luo, *et al.*, Nitrogen fixation sustained productivity in the wake of the Palaeoproterozoic Great Oxygenation Event. *Nat. Commun.* **9**, 978 (2018).

32. J. F. Stolz, P. Basu, Evolution of nitrate reductase: molecular and structural variations on a common function. *Chembiochem* **3**, 198–206 (2002).

33. P. Sánchez-Baracaldo, J. A. Raven, D. Pisani, A. H. Knoll, Early photosynthetic eukaryotes inhabited low-salinity habitats. *Proc. Natl. Acad. Sci. U. S. A.* **114**, E7737–E7745 (2017).

34. H. C. Betts, *et al.*, Integrated genomic and fossil evidence illuminates life's early evolution and eukaryote origin. *Nat. Ecol. Evol.* **2**, 1556–1562 (2018).

35. S. M. Porter, Insights into eukaryogenesis from the fossil record. *Interface Focus* **10**, 20190105 (2020).

36. J. F. H. Strassert, I. Irisarri, T. A. Williams, F. Burki, A molecular timescale for eukaryote evolution with implications for the origin of red algal-derived plastids. *Nat. Commun.* **12**, 1879 (2021).

37. P. A. Cohen, R. B. Kodner, The earliest history of eukaryotic life: uncovering an evolutionary story through the integration of biological and geological data. *Trends Ecol. Evol.* **37**, 246–256 (2022).

38. T. A. Mahendrarajah, *et al.*, ATP synthase evolution on a cross-braced dated tree of life. *Nat. Commun.* **14**, 7456 (2023).

39. J. M. Craig, S. Kumar, S. B. Hedges, The origin of eukaryotes and rise in complexity were synchronous with the rise in oxygen. *Front. Bioinform.* **3**, 1233281 (2023).

40. B. Schmid, *et al.*, Biochemical and structural characterization of the cross-linked complex of nitrogenase: comparison to the ADP-$AlF_4^{(-)}$-stabilized structure. *Biochemistry* **41**, 15557–15565 (2002).

41. T. Spatzal, *et al.*, Evidence for interstitial carbon in nitrogenase FeMo cofactor. *Science* **334**, 940 (2011).

42. D. Sippel, O. Einsle, The structure of vanadium nitrogenase reveals an unusual bridging ligand. *Nat. Chem. Biol.* **13**, 956–960 (2017).

43. C. Trncik, F. Detemple, O. Einsle, Iron-only Fe-nitrogenase underscores common catalytic principles in biological nitrogen fixation. *Nat. Catal.* **6**, 415–424 (2023).

44. C. M. Ostrander, A. C. Johnson, A. D. Anbar, Earth's First Redox Revolution. *Annu.*

Rev. Earth Planet. Sci. **49**, 337–366 (2021).

45. C. Scott, *et al.*, Tracing the stepwise oxygenation of the Proterozoic ocean. *Nature* **452**, 456–459 (2008).

46. T. W. Lyons, C. T. Reinhard, N. J. Planavsky, The rise of oxygen in Earth's early ocean and atmosphere. *Nature* **506**, 307–315 (2014).

47. A. D. Anbar, Oceans. Elements and evolution. *Science* **322**, 1481–1483 (2008).

48. E. K. Moore, J. Hao, S. J. Spielman, N. Yee, The evolving redox chemistry and bioavailability of vanadium in deep time. *Geobiology* **18**, 127–138 (2020).

49. R. Tostevin, I. A. M. Ahmed, Micronutrient availability in Precambrian oceans controlled by greenalite formation. *Nat. Geosci.* 1–6 (2023). https://doi.org/10.1038/s41561-023-01294-0.

50. M. C. Koehler, R. Buick, M. A. Kipp, E. E. Stüeken, J. Zaloumis, Transient surface ocean oxygenation recorded in the ~2.66-Ga Jeerinah Formation, Australia. *Proc. Natl. Acad. Sci. U. S. A.* **115**, 7711–7716 (2018).

51. J. Monod, The growth of bacterial cultures. *Annu. Rev. Microbiol.* **3**, 371–394 (1949).

52. S. Sharma, R. Steuer, Modelling microbial communities using biochemical resource allocation analysis. *J. R. Soc. Interface* **16**, 20190474 (2019).

53. A. Quigg, A. J. Irwin, Z. V. Finkel, Evolutionary inheritance of elemental stoichiometry in phytoplankton. *Proc. Biol. Sci.* **278**, 526–534 (2011).

54. D. Tilman, Resources: A graphical-mechanistic approach to competition and predation. *Am. Nat.* **116**, 362–393 (1980).

55. S. Dutkiewicz, M. J. Follows, J. G. Bragg, Modeling the coupling of ocean ecology and biogeochemistry. *Global Biogeochem. Cycles* **23** (2009).

56. B. A. Ward, S. Dutkiewicz, C. M. Moore, M. J. Follows, Iron, phosphorus, and nitrogen supply ratios define the biogeography of nitrogen fixation. *Limnol. Oceanogr.* **58**, 2059–2075 (2013).

57. A. Landolfi, *et al.*, Can top-down controls expand the ecological niche of marine N2 fixers? *Front. Microbiol.* **12**, 690200 (2021).

58. C. Tuit, J. Waterbury, G. Ravizza, Diel variation of molybdenum and iron in marine diazotrophic cyanobacteria. *Limnol. Oceanogr.* **49**, 978–990 (2004).

59. J. B. Glass, F. Wolfe-Simon, J. J. Elser, A. D. Anbar, Molybdenum-nitrogen co-limitation in freshwater and coastal heterocystous cyanobacteria. *Limnol. Oceanogr.* **55**, 667–676 (2010).

60. J.-P. Bellenger, T. Wichard, Y. Xu, A. M. L. Kraepiel, Essential metals for nitrogen fixation in a free-living N_2-fixing bacterium: chelation, homeostasis and high use efficiency: Homeostasis of nitrogenase metal cofactors inA. vinelandii. *Environ. Microbiol.* **13**, 1395–1411 (2011).

61. A. C. Redfield, The biological control of chemical factors in the environment. *Sci. Prog.* **11**, 150–170 (1960).

62. J. I. Sprent, J. A. Raven, Evolution of nitrogen-fixing symbioses. *Proc., Sect. B Biol. Sci.* **85**, 215–237 (1985).

63. J. A. Raven, The iron and molybdenum use efficiencies of plant growth with different energy, carbon and nitrogen sources. *New Phytol.* **109**, 279–287 (1988).

64. T. Großkopf, J. Laroche, Direct and indirect costs of dinitrogen fixation in Crocosphaera watsonii WH8501 and possible implications for the nitrogen cycle. *Front. Microbiol.* **3**, 236 (2012).

65. M. Pahlow, H. Dietze, A. Oschlies, Optimality-based model of phytoplankton growth and diazotrophy. *Mar. Ecol. Prog. Ser.* **489**, 1–16 (2013).

66. K. A. Turk-Kubo, *et al.*, In situ diazotroph population dynamics under different resource ratios in the north pacific subtropical gyre. *Front. Microbiol.* **9**, 1616 (2018).

67. J. B. Glass, F. Wolfe-Simon, A. D. Anbar, Coevolution of metal availability and nitrogen assimilation in cyanobacteria and algae. *Geobiology* **7**, 100–123 (2009).

68. D. Tilman, Resource competition and community structure. *Monogr. Popul. Biol.* **17**, 1–296 (1982).

69. A. M. Grunden, K. T. Shanmugam, Molybdate transport and regulation in bacteria. *Arch. Microbiol.* **168**, 345–354 (1997).

70. L. J. Liermann, R. L. Guynn, A. Anbar, S. L. Brantley, Production of a molybdophore during metal-targeted dissolution of silicates by soil bacteria. *Chem. Geol.* **220**, 285–302 (2005).

71. M. Tejada-Jiménez, A. Llamas, E. Sanz-Luque, A. Galván, E. Fernández, A high-affinity molybdate transporter in eukaryotes. *Proc. Natl. Acad. Sci. U. S. A.* **104**, 20126–20130 (2007).

72. J. P. Bellenger, T. Wichard, A. B. Kustka, A. M. L. Kraepiel, Uptake of molybdenum and vanadium by a nitrogen-fixing soil bacterium using siderophores. *Nat. Geosci.* **1**, 243–246 (2008).

73. J. B. Glass, R. P. Axler, S. Chandra, C. R. Goldman, Molybdenum limitation of microbial nitrogen assimilation in aquatic ecosystems and pure cultures. *Front. Microbiol.* **3**, 331 (2012).

74. M. Navarro-Rodríguez, J. M. Buesa, L. M. Rubio, Genetic and biochemical analysis of the Azotobacter vinelandii molybdenum storage protein. *Front. Microbiol.* **10**, 579 (2019).

75. J. P. Bellenger, R. Darnajoux, X. Zhang, A. M. L. Kraepiel, Biological nitrogen fixation by alternative nitrogenases in terrestrial ecosystems: a review. *Biogeochemistry* **149**, 53–73 (2020).

76. B. S. Twining, S. B. Baines, The trace metal composition of marine phytoplankton. *Ann. Rev. Mar. Sci.* **5**, 191–215 (2013).